Analytica Chimica Acta 1146 (2021) 70–76

Contents lists available at ScienceDirect

Analytica Chimica Acta

journal homepage: www.elsevier.com/locate/aca

Rapid electrochemical-biosensor microchip platform for determination of microalbuminuria in CKD patients

Chin-Chung Tseng [a, 1], Chien-Hsuan Ko [b, 1], Song-Yu Lu [b], Chia-En Yang [c], Lung-Ming Fu [b, d, *], Chi-Yu Li [b]

[a] Department of Internal Medicine, College of Medicine, National Cheng Kung University and Hospital, Tainan, 704, Taiwan
[b] Department of Engineering Science, National Cheng Kung University, Tainan, 701, Taiwan
[c] Office of Physical Education, National Pingtung University of Science and Technology, Pingtung, 912, Taiwan
[d] Graduate Institute of Materials Engineering, National Pingtung University of Science and Technology, Pingtung, 912, Taiwan

HIGHLIGHTS

- An EC-biosensor microchip system is presented for detection of urinary MAU concentration.
- An electroactive substance of amaranth is used to modify the surface of the sensing electrodes.
- The MAU concentration in the urine of 82 adult CKD patients was measured.
- The measurement results are in good agreement (R^2 = 0.988) with the official method.

GRAPHICAL ABSTRACT

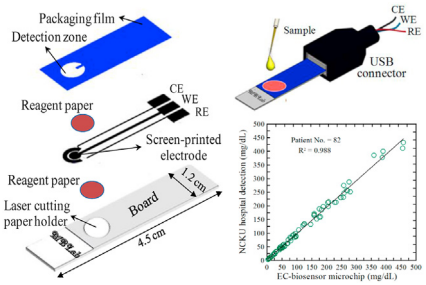

ARTICLE INFO

Article history:
Received 11 November 2020
Received in revised form
11 December 2020
Accepted 15 December 2020
Available online 21 December 2020

Keywords:
Electrochemical biosensor
Microchip
Microalbuminuria
Albumin
Chronic kidney disease

ABSTRACT

An electrochemical-biosensor (EC-biosensor) microchip consisting of screen-printed electrodes and a double-layer reagent paper detection zone impregnated with amaranth is proposed for the rapid determination of microalbuminuria (MAU) in human urine samples. Under the action of an applied deposition potential, the amaranth is adsorbed on the electrode surface and the subsequent reaction between the modified surface and the MAU content in the urine sample prompts the formation of an inert layer on the electrode surface. The inert layer impedes the transfer of electrons and hence produces a drop in the response peak current, from which the MAU concentration can then be determined. The measurement results obtained for seven artificial urine samples with known MAU concentrations in the range of 0.1–40 mg/dL show that the measured response peak current is related to the MAU concentration with a determination coefficient of R^2 = 0.991 in the low concentration range of 0.1–10 mg/dL and R^2 = 0.996 in the high concentration range of 10–40 mg/dL. Furthermore, the detection results obtained for 82 actual chronic kidney disease (CKD) patients show an excellent agreement (R^2 = 0.988) with the hospital analysis results. Overall, the results confirm that the proposed detection platform provides a convenient and reliable approach for performing sensitive point-of-care testing (POCT) of the MAU content in human urine samples.

1. Introduction

Microalbuminuria (MAU) is an extremely important indicator for the early detection of kidney disease and is often associated

* Corresponding author. Department of Engineering Science, National Cheng Kung University, Tainan, 701, Taiwan.
E-mail address: loudyfu@mail.ncku.edu.tw (L.-M. Fu).
[1] These authors contributed equally to this paper.

https://doi.org/10.1016/j.aca.2020.12.029
0003-2670/

with an increased incidence of metabolic syndrome, insulin resistance, obesity, hypertension, dyslipidemia, and kidney and cardiovascular diseases. MAU is usually not present in urine, or the measured value is less than 3 mg/dL, because albumin is retained in the blood by the kidneys in a functioning body. Many studies have pointed out that under the influence of certain diseases; the renal albumin excretion rate may increase, thereby increasing the amount of albumin discharged in the urine [1,2]. Clinically, MAU is defined as a urine albumin excretion of 30–300 mg/day from a 24-h urine collection, or 3–30 mg/dL from a random or first morning urine collection. The excretion of albumin in urine is in the range of 30–300 mg/dL is called albuminuria [3]. Urine albumin is a reliable indicator of many human diseases, including kidney disease, cardiovascular disease, and diabetes [4]. As a result, developing effective methods for the early detection of MAU is of great clinical importance.

Due to the low characteristic concentration of MAU in human biological samples, it is difficult to quantify the concentration level using general biochemical detection methods such as spectrophotometery and colorimetric methods. Accordingly, the literature contains many proposals for more specific methods for MAU determination, including immunoturbidimetry [5], immunoassays [1,2], liquid chromatography [6], spectrophotometery [7], and microfluidic devices [8]. However, these methods are generally impractical for point-of-care (POC) assays due to their long response time, narrow linear range, high susceptibility to interference, need for professional technical operators, and requirement for expensive and complex detection instruments.

Microfluidic lab-on-a-chip systems [9–17] combine knowledge in various fields, such as mechanics, physics, chemistry, biology and medicine, and have significant advantages for POC testing (POCT), including a rapid response, a low sample volume, high sensitivity, high portability and low cost. The literature contains many micro-total analysis systems (μTAS) [18–25] and microfluidic paper-based analysis devices (μPAD) [26–44] for a wide variety of applications. In recent years, microfluidic platforms have been used to detect total protein (TP) [45–47], the albumin/creatine ratio (ACR) [48,49], albumin (ALB) [50–56] and microalbuminuria MAU [57,58] in blood or urine samples. However, while these methods usually have no problem in detecting TP and ALB in blood samples, or ALB and ACR in urine samples, the detection of MAU in urine samples remains a significant challenge due to its low concentration and wide range. Nonetheless, the detection of MAU in urine samples is a matter of great clinical concern due to the usefulness of MAU as a biomarker for a large number of human diseases. Consequently, the problem of developing effective microfluidic platforms for the determination of MAU in urine samples continues to attract great interest in the literature. For example, the authors in Refs. [57,58] combined the field amplification stacking method with the use of electric field and pH gradients to enhance the concentration of MAU and improve the colorimetric detection performance as a result. The experimental results showed that both devices were capable of detecting MAU in artificial urine samples with concentrations as low as 1–30 mg/dL.

The present study develops an EC-biosensor microchip consisting of a double-layer reagent paper detection zone and screen-printed electrodes for the rapid determination of microalbuminuria (MAU) in human urine samples. In the proposed device, amaranth (an electroactive substance) is adsorbed on the surface of the electrodes under the effects of an external potential and subsequently reacts with the MAU content in the urine sample. The reaction process results in the formation of an inert layer on the electrode surface, which leads to a reduction in the response current from which the MAU concentration can then be inversely derived. The feasibility of the proposed device is demonstrated using both artificial urine samples with known MAU concentrations and real-world samples taken from CKD patients with MAU concentration levels ranging from 0 to 450 mg/dL.

2. Materials and methods

2.1. Chemical and reagent preparation

Albumin control samples were purchased from Sigma-Aldrich (Germany). Artificial urine solutions (pH 6.6) were obtained from Pickering (USA). A phosphate buffered saline (PBS) solution with pH 6 was prepared consisting of 1.835 g Na_2HPO_4 and 5.955 g NaH_2PO_4 mixed with 0.15 M sodium chloride (NaCl, 99.5%) and deionized (DI) water. A 0.01 M amaranth solution was prepared by dissolving 0.08 g of amaranth powder (Echo Chemical Co. Ltd., Taiwan) in 10 mL of PBS solution. Similarly, a 0.1 M potassium ferricyanide solution was prepared by dissolving 3.293 g of potassium ferricyanide powder (Showa Corp., Japan) in 10 mL of potassium chloride buffer. Control samples with urinary MAU concentrations in the range of 0.1–40 mg/dL were prepared by diluting the stock solution with an appropriate quantity of PBS. Finally, real urine samples were collected from CKD patients at a university in southern Taiwan (National Cheng Kung University Hospital, Tainan, Taiwan). The preparation of real urine samples was centrifuged at 5000 rpm for 5 min to obtain the supernatant, and then diluted 10-fold with PBS solution as the detection sample solution.

2.2. Fabrication of EC-biosensor microchip and experimental setup

Fig. 1 shows a schematic diagram of the EC-biosensor microchip assembly process and subsequent urinary MAU concentration detection procedure. As shown in Fig. 1(a), filter paper was infiltrated in amaranth solution for 5 min to ensure that the solution was completely absorbed into the pore structure of filter paper. The reagent paper was then baked in an oven at 40 °C for 30 min to dry the solvent. The dried paper was cut into circular detection zones with a diameter of 5 mm using a CO_2 laser (see Fig. 1(b)). Three electrodes (based on silver flakes, graphite powder and dielectric materials) were printed on cardboard using a semi-automatic screen-printer. Two circular reagent papers were placed above and below the ends of the counter (CE) and working (WE) electrodes in the detection zone. Finally, the reagent papers and electrodes were assembled into the EC-biosensor microchip using packaging film (see Fig. 1(c)). For the double-layer reagent, each layer of reagent paper has the same composition. The purpose of using two layers of reagent paper is to increase the contact area between the EC-biosensor electrodes and the reactant, and to enhance the sensitivity of detection. For a more detailed description of sensitivity, please refer to section S.1 of the supplementary material. Following the fabrication process, the microchip was stored in a nitrogen environment at a temperature of 4 °C until required for use. To facilitate the MAU concentration detection process, the EC-biosensor was integrated with a self-made three-electrode cable USB connector (Fig. 1(d)) and then inserted into an electrochemical analyzer (CHI 611, CH Instruments Co., USA) (Fig. 1(e)). In the design of the three-electrode cable USB connector, use the three contacts in the USB socket as the connection of CE, WE and reference electrode (RE). The detailed design of the three-electrode cable USB connector is shown in Fig. S2 (see Supplementary Material).

Fig. 2 presents a schematic illustration of the detection principle employed in the proposed device. As described above, amaranth-impregnated reagent papers were adhered to the upper and lower surfaces of the WE and CE electrodes. 4 mM potassium

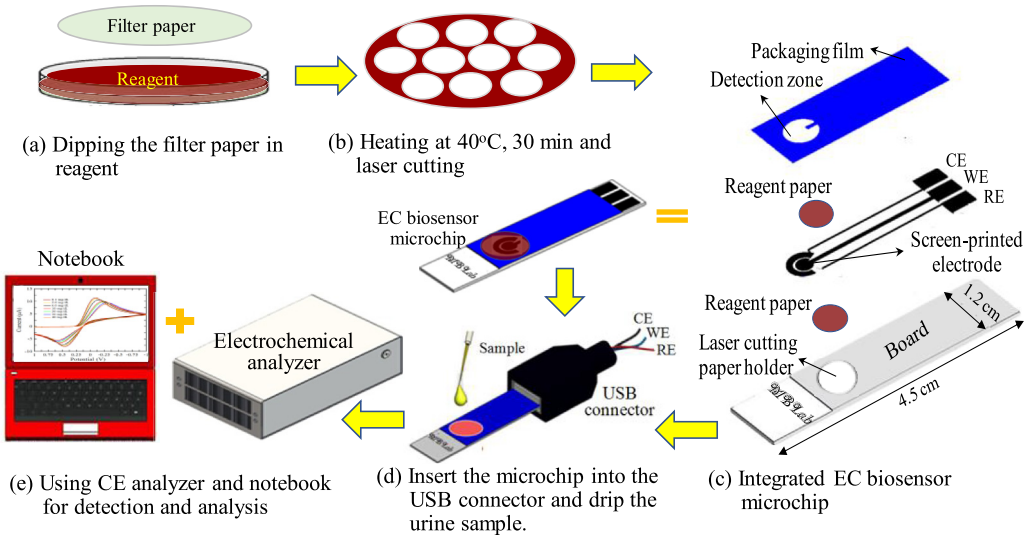

Fig. 1. Schematic illustration of EC-biosensor microchip platform and associated MAU concentration detection procedure.

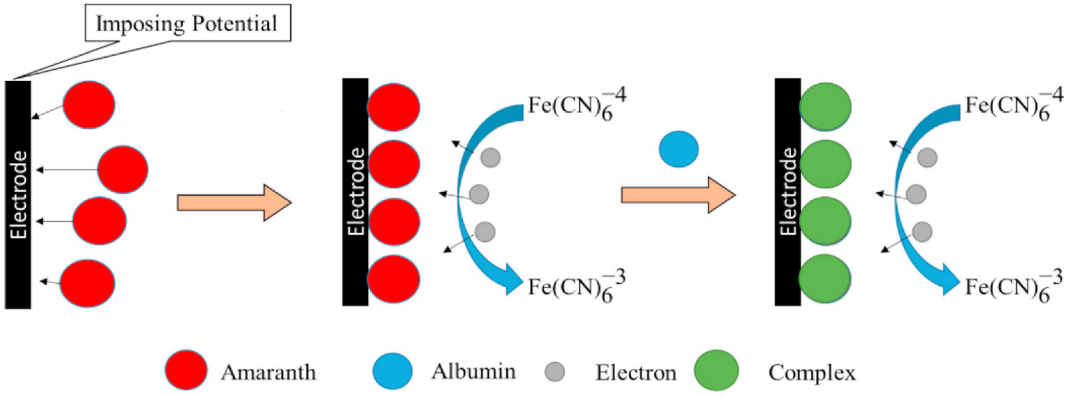

Fig. 2. Schematic diagram showing reaction principle of microchip platform.

ferricyanide solution was dropped on the reagent paper and a potential was applied for 1 min to adsorb the amaranth onto the electrode surface through a redox reaction. In the subsequent detection process, the MAU content in the urine sample (2 μL) interacted with the amaranth on the electrode surface to generate electrically-inert molecules, which led to an increase in the electron transfer resistance and a measurable decrease in the response current. Amaranth–ALB complex reduces the activity of Amaranth due to the combination of hydrogen bonds [59,60], causing it to generate electrically inert molecules and hinder electron transfer to the electrode surface, as shown in Fig. S3 (see Supplementary Material). A quantitative analysis of the MAU concentration was then obtained via cyclic voltammetry, as shown in Fig. 1(e)).

3. Results and discussions

3.1. Effect of deposition potential and potassium ferricyanide concentration on adsorption of amaranth

As described above, the amaranth ions are attracted to the surface of the electrode via an external potential and then react with the MAU in the urine sample to form an electrically-inert substance. In practice, the resolution of the detection process depends on the quantity of amaranth ions adsorbed on the electrode surface, which depends in turn on the magnitude of the deposition potential. Fig. 3(a) shows the effect of the deposition potential on the current inhibition effect of the amaranth for deposition potentials in the range of 0–0.8 V, 4 mM potassium ferricyanide, 0.25 mM amaranth and 20 mg/dL MAU. It is seen that the maximum current response occurs at 0.1 V, which indicates that a large amount of potassium ferricyanide is adsorbed on the electrode surface. In other words, the corresponding redox reaction greatly increases the current, and hence the potential of 0.1 V corresponds to the optimal deposition potential of potassium ferricyanide. However, a further inspection of Fig. 3(a), shows that the minimal current response occurs at 0.3 V. Thus, it is inferred that the optimal current suppression effect (i.e., the maximum formation of an electrically-inert layer on the electrode surface) is obtained using a deposition potential of 0.3 V.

Fig. 3(b) shows the current response of the EC-microchip for potassium ferricyanide solution concentrations of 1–6 mM, a deposition potential of 0.3 V, an amaranth concentration of 0.25 mM, and a MAU concentration of 20 mg/dL. For a potassium ferricyanide concentration of less than 4 mM, the current response increases with an increasing potassium ferricyanide concentration. In other words, the amaranth is not fully adsorbed on the electrode surface. However, as the potassium ferricyanide concentration increases beyond 4 mM, the current response remains almost

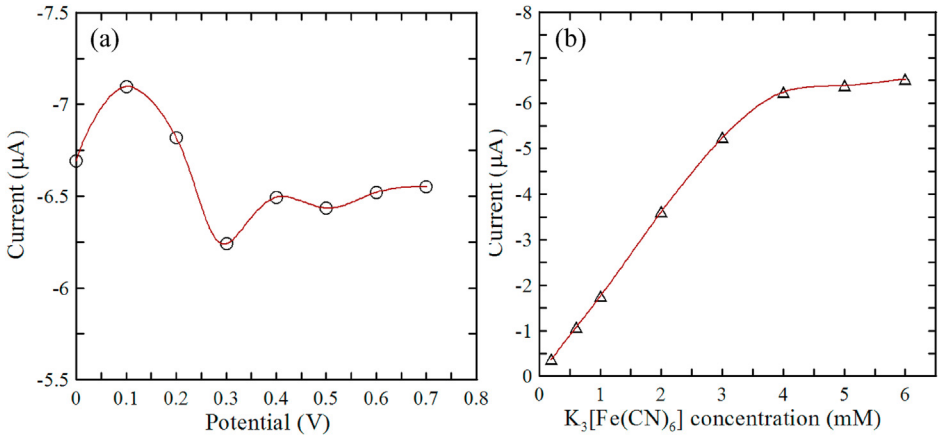

Fig. 3. (a) Effect of deposition potential on adsorption of amaranth on electrode surface and resulting inhibition of current. (b) Effect of potassium ferricyanide concentration on response peak current.

unchanged. In other words, the amaranth and MAU fully react to form an inert layer on the electrode surface, which impedes the transfer of electrons and therefore causes the current to saturate. Consequently, the potassium ferricyanide concentration was set as 4 mM in all of the remaining experiments.

3.2. Effect of amaranth concentration

As described in Section 2.2, the MAU concentration is determined by measuring the change in the response peak current following the reaction between the adsorbed amaranth ions on the electrode surface and the MAU in the urine sample. Fig. 4(a) shows the variation of the response peak current with the MAU concentration given amaranth concentrations of 0.1, 0.25, 0.5 and 1.0 mM, respectively. (Note that in accordance with the results obtained in Section 3.1, the potassium ferricyanide concentration and deposition potential were set as 4 mM and 0.3 V, respectively.) As shown, the proposed device achieves a resolution of 20.68, 12.75, 15.02 and 20.34 mg/dL per μA for amaranth concentrations of 0.1, 0.25, 0.5 and 1.0 mM, respectively. In other words, an amaranth concentration of 0.25 mM maximizes the resolution of the EC-microchip for MAU concentration sensing. However, the linear determination coefficient values (R^2) of the detection curves obtained with different concentrations of amaranth are all less than 0.8. Hence, the reaction performance of different amaranth concentrations was further analyzed by spectrophotometry to confirm the optimal concentration. Fig. 4(b) shows the measured UV absorbance values of MAU samples with amaranth concentrations of 0.1 mM, 0.25 mM and 0.5 mM, respectively, given MAU concentrations of 0.1–30 mg/dL, a potassium ferricyanide concentration of 4 mM and an excitation wavelength of 524 nm. In this case, the linear determination coefficient values of the three detection curves are all greater than $R^2 = 0.98$. Furthermore, the corresponding resolution values are 140.2, 73.5 and 111.5 mg/dL per a.u., respectively. Thus, an amaranth concentration of 0.25 mM was confirmed as the optimal concentration for the remaining MAU detection experiments.

3.3. Calibration of detection platform

Overall, the optimal EC-biosensor detection parameters were found to be a potassium ferricyanide concentration of 4 mM, an amaranth concentration of 0.25 mM, a buffer solution condition of pH 6, a deposition potential of 0.3 V, and a deposition time of 60 s. The detection performance of the EC-biosensor prepared using these optimal parameters was calibrated by performing cyclic voltammetry tests using control samples with known MAU concentrations in the range of 0.1–40 mg/dL and a scanning rate of 0.1 V/s. Fig. 5(a) presents the corresponding results for a scanning range of −1 to 1 V. It is clearly seen that the peak current decreases as the MAU concentration increases as a result of the corresponding increase in the electron transmission impedance.

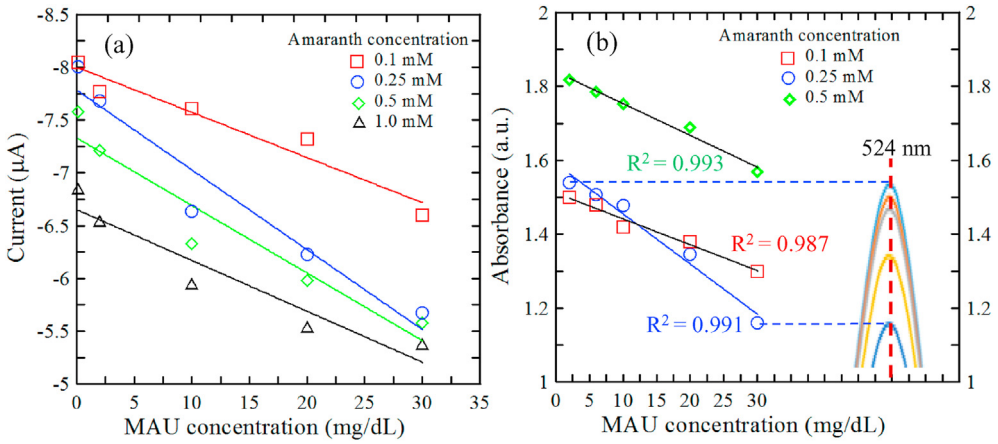

Fig. 4. (a) Response peak current and (b) UV absorbance as function of MAU concentration for different amaranth concentrations.

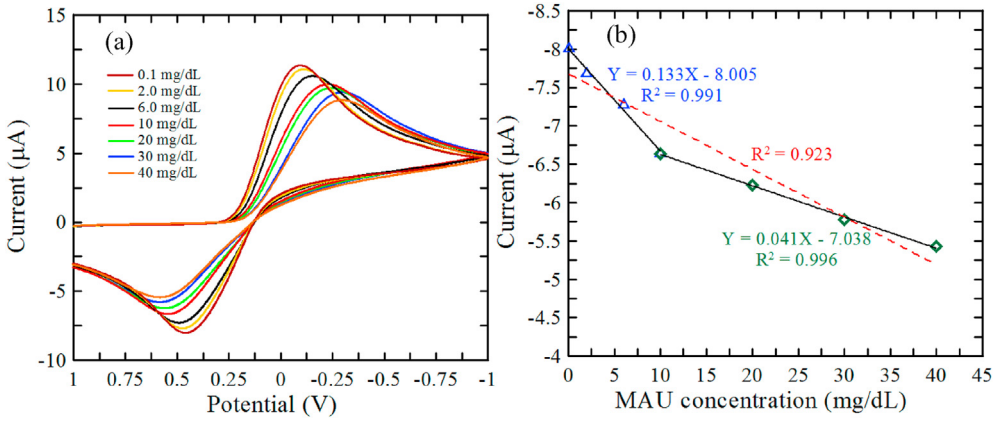

Fig. 5. (a) Cyclic voltammograms for different MAU concentrations given buffer solution with pH 6 and scanning rate of 0.1 V/s. (b) Response peak current as function of MAU concentration in range of 0.1–40 mg/dL.

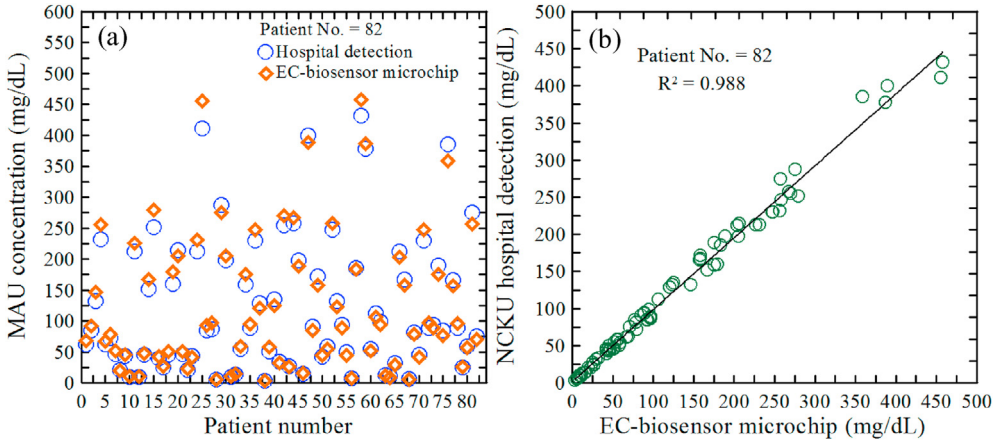

Fig. 6. Comparison of MAU detection results obtained using EC-biosensor microchip platform and NCKU Hospital standard analysis method.

Fig. 5(b) shows the variation of the response peak current with the MAU concentration over the considered range of 0.1–40 mg/dL. When evaluated over the full MAU concentration range, the determination coefficient has a value of $R^2 = 0.923$ (see red dashed line). However, it is observed that the regression line deviates significantly from the measured response peak current at an MAU concentration of 10 mg/dL. Thus, to improve the prediction performance, the fitting process was repeated separately for the MAU concentration ranges of 0.1–10 mg/dL and 10–40 mg/dL, respectively. The corresponding regression formulae were found to be $Y = 0.113\ X - 8.005$ and $Y = 0.041\ X - 7.038$, respectively, with determination coefficients (R^2) of 0.991 and 0.996, respectively. In two cases, the determination coefficient is approximately the ideal value of 1. Thus, the reliability of the two regression equations for predicting the MAU concentration from the detected response peak current is confirmed.

3.4. Detection performance of EC-biosensor for real-world MAU specimens

The practical feasibility of the EC-biosensor was evaluated using 82 real urine samples collected from CKD patients at National Cheng Kung University (NCKU) Hospital in southern Taiwan. Prior to testing, the urine samples were rapidly centrifuged using a self-developed micro-flow centrifugal device, filtered, mixed with 0.01 mM [$Sb(OH)_6$]] solution (remove sodium ions to reduce interference), and then filtered once again to extract the upper layer. For each sample, the MAU concentration was calculated by substituting the measured response peak current into the calibration curve equations derived in the previous section.

Fig. 6(a) compares the results obtained for the MAU concentrations of the 82 samples using the EC-biosensor microchip platform with those obtained using a standard analysis method (immunoturbidimetry). As shown in Fig. 6(b), the correlation coefficient between the two set of results has a value of $R^2 = 0.988$. Moreover, the recovery rate of the 82 samples is equal to 102.6% (±7.2%). The applicability of the EC-biosensor platform for MAU concentration detection was further investigated over the specific concentration ranges of 0–30 mg/dL (microalbuminuria) and 30–300 mg/dL (albuminuria), as shown in Fig. 7(a) and (b), respectively. As shown, the corresponding correlation coefficients (R^2) are 0.977 and 0.985, respectively. In other words, the reliability of the detection results is confirmed. Moreover, the detection limit of the proposed device is confirmed to be 0.1 mg/dL.

4. Conclusion

This study has presented a highly-sensitive EC-biosensor microchip platform for the rapid and accurate measurement of the MAU concentration in human urine samples. In the proposed device, an electroactive substance (amaranth) is used to modify the surface of the sensing electrodes, and subsequently reacts with the

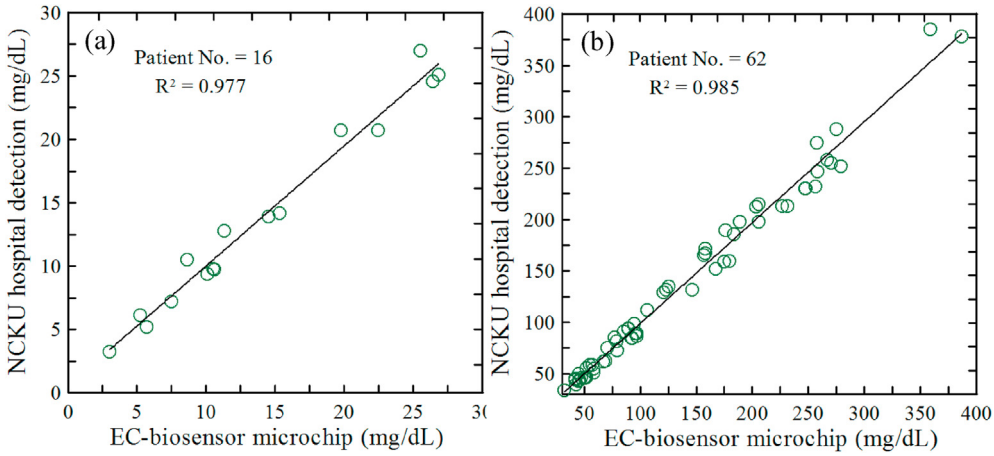

Fig. 7. Comparison of detection results obtained using EC-biosensor microchip platform and NCKU Hospital standard analysis method for patients with MAU concentration ranges of (a) 0–30 mg/dL (microalbuminuria) and (b) 30–300 mg/dL (albuminuria).

MAU content of the urine sample to form an electrically-inert reaction layer on the electrode surface. The reaction layer impedes the transfer of electrons and hence results in a reduction in the current response from which the MAU concentration can then be inversely derived. The experimental results obtained for seven artificial urine samples with known MAU concentrations in the range of 0.1–40 mg/dL have shown that the crrent platform has a determination coefficient (R^2) of 0.991 in the low concentration range (0.1–10 mg/dL) and 0.996 in the high concentration range (10–40 mg/dL). Moreover, the device has a detection limit of 0.1 mg/dL. It has been shown that the MAU concentration measurements obtained using the proposed device for 82 real-world CKD patient samples are in good agreement (R^2 = 0.988) with the results obtained using an official macroscopic measurement method. In addition, the recovery rate is 102.6% (±7.2%). Hence, the overall feasibility of the proposed EC-biosensor microchip platform for practical clinical purposes is confirmed.

CRediT authorship contribution statement

Chin-Chung Tseng: Data curation, Writing - original draft, preparation, and, Supervision. **Chien-Hsuan Ko:** Investigation, Methodology, Software, and, Data curation. **Song-Yu Lu:** Investigation, Methodology, Software, and, Data curation. **Chia-En Yang:** and. **Lung-Ming Fu:** Data curation, Writing - original draft, preparation, and, Supervision. **Chi-Yu Li:** Writing - review & editing, Investigation.

Declaration of competing interest

The authors declare that they have no known competing financial interests or personal relationships that could have appeared to influence the work reported in this paper.

Acknowledgement

The authors would like to thank the Ministry of Science and Technology of Taiwan for the financial support of this study under Grant Nos. MOST 106-2314-B-006-085- MY3, MOST 106-2221-E-006-253-MY3, MOST 108-2622-E -006-026-CC, and MOST 109-2221-E-006 -043 -MY3.

Appendix A. Supplementary data

Supplementary data to this article can be found online at https://doi.org/10.1016/j.aca.2020.12.029.

References

[1] Z. Huang, R. Zhang, H. Chena, W. Weng, Q. Lin, D. Deng, Z. Li, J. Kong, Sensitive polydopamine bi-functionalized SERS immunoassay for microalbuminuria detection, Biosens. Bioelectron. 142 (2019) 111542.
[2] M.O. Shaikh, P. Zhu, C.C. Wang, Y.C. Du, C.H. Chuang, Electrochemical immunosensor utilizing electrodeposited Au nanocrystals and dielectrophoretically trapped PS/Ag/ab-HSA nanoprobes for detection of microalbuminuria at point of care, Biosens. Bioelectron. 126 (2019) 572–580.
[3] J. Budhathoki-Uprety, J. Shah, J.A. Korsen, A.E. Wayne, T.V. Galassi, J.R. Cohen, J.D. Harvey, P.V. Jena, L.V. Ramanathan, E.A. Jaimes, D.A. Helle, Synthetic molecular recognition nanosensor paint for microalbuminuria, Nat. Commun. 10 (2019) 3605.
[4] T. Assulyn, R. Khamisy-Farah, W. Nseir, A. Bashkin, R. Farah, Neutrophil-to-lymphocyte ratio and red blood cell distribution width as predictors of microalbuminuria in type 2 diabetes, J. Clin. Lab. Anal. 34 (2020), e23259.
[5] V.R. Bhatt, V.B. Khese, S.L. Jadhav, A.L. Kakrani, Urinary albumin excretion, estimated glomerular filtration rate, and prevalence of microalbuminuria in obese nondiabetic and nonhypertensive adults: a cross-sectional study, Indian J. Nephrol. 29 (2019) 166–171.
[6] J.Z. Tsai, C.J. Chen, K. Settu, Y.F. Lin, C.L. Chen, J.T. Liu, Screen-printed carbon electrode-based electrochemical immunosensor for rapid detection of microalbuminuria, Biosens. Bioelectron. 77 (2016) 1175–1182.
[7] C.K. Chou, Y.T. Lee, S.M. Chen, C.W. Hsieh, T.C. Huang, Y.C. Li, J.A. Lee, Elevated urinary d-lactate levels in patients with diabetes and microalbuminuria, J. Pharmaceut. Biomed. Anal. 116 (2015) 65–70.
[8] C.C. Lin, J.L. Hsu, C.C. Tseng, G.B. Lee, An integrated microfluidic system for the determination of microalbuminuria by measuring the albumin-to-creatinine ratio, Microfluid. Nanofluidics 10 (2011) 1055–1067.
[9] C.Y. Lee, L.M. Fu, Recent advances and applications of micromixers, Sensor. Actuator. B Chem. 259 (2018) 677–702.
[10] S. Marsousi, J. Karimi-Sabet, M.A. Moosavian, Y. Amini, Liquid-liquid extraction of calcium using ionic liquids in spiral microfluidics, Chem. Eng. J. 356 (2019) 492–505.
[11] L. Li, X. Liu, J. Xu, C. Kan, Microfluidic preparation of thiol-containing monodisperse polymer microspheres and their adsorption of Pb^{2+} in water, Chem. Eng. J. 375 (2019) 122012.
[12] L.A.N. Dayao, C.C. Liu, S.Y. Hsu, L.L. Tayo, W.J. Ju, L.M. Fu, Multifunctional microchip-based distillation apparatus II-Aerated distillation for sulfur dioxide detection, Anal. Chim. Acta 1071 (2019) 44–52.
[13] S.Y. Hsu, C.C. Liu, C.E. Yang, L.M. Fu, Multifunctional microchip-based distillation apparatus I-Steam distillation for formaldehyde detection, Anal. Chim. Acta 1062 (2019) 94–101.
[14] Y.T. Wu, C.E. Yang, C.H. Ko, Y.N. Wang, C.C. Liu, L.M. Fu, Microfluidic detection platform with integrated micro-spectrometer system, Chem. Eng. J. 393 (2020) 124700.
[15] H. Liu, M. Jie, Z. He, H.F. Li, J.M. Lin, Study of antioxidant effects on malignant glioma cells by constructing a tumor-microvascular structure on microchip, Anal. Chim. Acta 978 (2017) 1–9.
[16] C.T. Kung, H. Gao, C.Y. Lee, Y.N. Wang, W. Dong, C.H. Ko, G. Wang, L.M. Fu, Microfluidic synthesis control technology and its application in drug delivery,

bioimaging, biosensing, environmental analysis and cell analysis, Chem. Eng. J. 399 (2020) 125748.
[17] J. Chen, H. Li, H. Xie, D. Xu, A novel method combining aptamer-Ag_{10}NPs based microfluidic biochip with bright field imaging for detection of KPC-2-expressing bacteria, Anal. Chim. Acta 1132 (2020) 20–27.
[18] H. Shi, K. Nie, B. Dong, M. Long, H. Xu, Z. Liu, Recent progress of microfluidic reactors for biomedical applications, Chem. Eng. J. 361 (2019) 635–650.
[19] X. Wang, L. Deng, B.T. Gjertsen, A microfluidic device for differential capture of heterogeneous rare tumor cells with epithelial and mesenchymal phenotypes, Anal. Chim. Acta 1129 (2020) 1–11.
[20] S.C. Chen, C. C Liu, Y.N. Wang, L.M. Fu, S.H. Shih, An integrated microfluidic loop-mediated isothermal amplification platform for koi herpesvirus detection, Chem. Eng. J. 334 (2018) 1828–1834.
[21] Z. Wu, Y. Zheng, L. Lin, S. Mao, Z. Li, J.M. Lin, Controllable synthesis of multicompartmental particles using 3D microfluidics, Angew. Chem. Int. Ed. 59 (2020) 2225–2229.
[22] W. He, Y. Gao, G. Zhu, H. Wu, Z. Fang, K. Guo, Microfluidic synthesis of fatty acid esters: integration of dynamic combinatorial chemistry and scale effect, Chem. Eng. J. 381 (2020) 122721.
[23] Y. Cai, J.C. Niu, Y.Q. Liu, X.L. Du, Z.Y. Wu, Online sample clean-up and enrichment of proteins from salty media with dynamic double gradients on a paper fluidic channel, Anal. Chim. Acta 1100 (2020) 149–155.
[24] J. Yang, Y. Zhu, F. Wang, L. Deng, X. Xu, W. Cui, Microfluidic liposomes-anchored microgels as extended delivery platform for treatment of osteoarthritis, Chem. Eng. J. 400 (2020) 126004.
[25] W. Zhang, N. Li, L. Lin, Q. Huang, K. Uchiyama, J.M. Lin, Concentrating single cells in picoliter droplets for phospholipid profiling on a microfluidic system, Small 16 (2020) 1903402.
[26] L.M. Fu, C.C. Liu, C.E. Yang, Y.N. Wang, C.H. Ko, A PET/paper chip platform for high resolution sulphur dioxide detection in foods, Food Chem. 286 (2019) 316–321.
[27] C.C. Liu, Y.N. Wang, L.M. Fu, D.Y. Yang, Rapid integrated microfluidic paper-based system for sulfur dioxide detection, Chem. Eng. J. 316 (2017) 790–796.
[28] C.C. Liu, Y.N. Wang, L.M. Fu, Y.H. Huang, Microfluidic paper-based chip platform for formaldehyde concentration detection, Chem. Eng. J. 332 (2018) 695–701.
[29] C.C. Tseng, R.J. Yang, W.J. Ju, L.M. Fu, Microfluidic paper-based platform for whole blood creatinine detection, Chem. Eng. J. 348 (2018) 117–124.
[30] S. Kumar, M. Umar, A. Saifi, S. Kumar, S. Augustine, S. Srivastava, B.D. Malhotra, Electrochemical paper based cancer biosensor using iron oxide nanoparticles decorated PEDOT:PSS, Anal. Chim. Acta 1056 (2019) 135–145.
[31] C.T. Kung, C.Y. Hou, Y.N. Wang, L.M. Fu, Microfluidic paper-based analytical devices for environmental analysis of soil, air, ecology and river water, Sensor. Actuator. B Chem. 301 (2019) 126855.
[32] X. Fu, B. Xia, B. Ji, S. Lei, Y. Zhou, Flow controllable three-dimensional paper-based microfluidic analytical devices fabricated by 3D printing technology, Anal. Chim. Acta 1065 (2019) 64–70.
[33] M. Taghizadeh-Behbahani, B. Hemmateenejad, M. Shamsipur, A. Tavassoli, A paper-based length of stain analytical device for naked eye (readout-free) detection of cystic fibrosis, Anal. Chim. Acta 1080 (2019) 138–145.
[34] T. Zangmo, A. Siripinyanond, Exploring the applicability of nano-selenium for capture of mercury vapor: paper based sorbent and a chemical modifier in graphite furnace atomic absorption spectrometry, Anal. Chim. Acta 1085 (2019) 29–38.
[35] B.S. Batule, Y. Seok, M.G. Kim, An innovative paper-based device for DNA extraction from processed meat products, Food Chem. 321 (2020) 126708.
[36] W. Shi Huang, J. Li, N. Bao, C. Yu, H. Gu, Determination of salivary uric acid by using poly(3,4-ethylenedioxythipohene) and graphene oxide in a disposable paper-based analytical device, Anal. Chim. Acta 1103 (2020) 75–83.
[37] L. Cao, G.C. Han, H. Xiao, Z. Chen, C. Fang, A novel 3D paper-based microfluidic electrochemical glucose biosensor based on rGO-TEPA/PB sensitive film, Anal. Chim. Acta 1096 (2020) 34–43.
[38] R. Caoa, Z. Panb, H. Tang, J. Wu, J. Tianc, A. Nilghazd, M. Li, Understanding the coffee-ring effect of red blood cells for engineering paper-based blood analysis devices, Chem. Eng. J. 391 (2020) 123522.
[39] E. Noviana, D.B. Carrão, R. Pratiwi, C.S. Henry, Emerging applications of paper-based analytical devices for drug analysis: a review, Anal. Chim. Acta 1116 (2020) 70–90.
[40] C.Y. Hou, L.M. Fu, W.J. Ju, P.Y. Wu, Microfluidic colorimetric system for nitrite detection in foods, Chem. Eng. J. 398 (2020) 125573.
[41] T. Akyazi, L. Basabe-Desmonts, F. Benito-Lopez, Review on microfluidic paper-based analytical devices towards commercialization, Anal. Chim. Acta 1001 (2018) 1–17.
[42] L. Wu, W. Zhang, C. Liu, M.F. Foda, Y. Zhu, Strawberry-like SiO2/Ag nanocomposites immersed filter paper as SERS substrate for acrylamide detection, Food Chem. 328 (2020) 127106.
[43] Y. Choi, M.K. Im, M.R. Lee, C.S. Kim, K.H. Lee, Highly sensitive enclosed multilayer paper-based microfluidic sensor for quantifying proline in plants, Anal. Chim. Acta 1105 (2020) 169–177.
[44] F. Li, M. You, S. Li, J. Hu, C. Liu, Y. Gong, H. Yang, F. Xu, Paper-based point-of-care immunoassays: recent advances and emerging trends, Biotechnol. Adv. 39 (2020) 107442.
[45] G.C. Bandara, C.A. Heist, V.T. Remcho, Patterned polycaprolactone-filled glass microfiber microfluidic devices for total protein content analysis, Talanta 176 (2018) 589–594.
[46] H. Gao, J.J. Liu, Y.Q. Liu, Z.Y. Wu, Detection of urine protein by a paper-based analytical device enhanced with ion concentration polarization effect, Microfluid. Nanofluidics 23 (2019) 51.
[47] R. Gao, Y. Wu, J. Huang, L. Song, H. Qian, X. Song, L. Cheng, R. Wang, L.b. Luo, G. Zhao, Development of a portable and sensitive blood serum test system using LED-based absorption photometry and pump-free microfluidic technology, Sensor. Actuator. B Chem. 286 (2019) 86–93.
[48] S. Chaiyo, K. Kalcher, A. Apilux, O. Chailapakul, W. Siangproh, A novel paper-based colorimetry device for the determination of the albumin to creatinine ratio, Analyst 143 (2018) 5453–5460.
[49] R. Hiraoka, K. Kuwahara, Y.C. Wen, T.H. Yen, Y. Hiruta, C.M. Cheng, D. Citterio, Based device for naked eye urinary albumin/creatinine ratio evaluation, ACS Sens. 5 (2020) 1110–1118.
[50] J. Wu, D. Tomsa, M. Zhang, P. Komenda, N. Tangri, C. Rigatto, F. Lin, A Passive mixing microfluidic urinary albumin chip for chronic kidney disease assessment, ACS Sens. 3 (2018) 2191–2197.
[51] R.J. Yang, C.C. Tseng, W.J. Ju, H.L. Wang, L.M. Fu, A rapid paper-based detection system for determination of human serum albumin concentration, Chem. Eng. J. 352 (2018) 241–246.
[52] R.J. Yang, C.C. Tseng, W.J. Ju, L.M. Fu, M.P. Syu, Integrated microfluidic paper-based system for determination of whole blood albumin, Sensor. Actuator. B Chem. 273 (2018) 1091–1097.
[53] P. Pokhrel, S. Jha, B. Giri, Selection of appropriate protein assay method for a paper microfluidics platform, Pract. Lab. Med. (2020), e00166.
[54] A.H. Imamura, T.P. Segato, L.J.M. de Oliveira, A. Hassan, F.N. Crespilho, E. Carrilho, Monitoring cellulose oxidation for protein immobilization in paper-based low-cost biosensors, Microchim. Acta 187 (2020) 272.
[55] Z. Luo, T. Lv, K. Zhu, Y. Li, L. Wang, J.J. Gooding, G. Liu, B. Liu, Paper-based ratiometric fluorescence analytical devices towards point-of-care testing of human serum albumin, Angew. Chem. Int. Ed. 59 (2020) 3131–3136.
[56] N. Mandal, S. Dutta, A. Gupta, D. Bandyopadhyay, Paper-based sensors for point-of-care kidney function monitoring, IEEE Sensor. J. 20 (2020) 9644–9651.
[57] Y. Cai, J.C. Niu, X.L. Du, F. Fang, Z.Y. Wu, Novel field amplification for sensitive colorimetric detection of microalbuminuria on a paper-based analytical device, Anal. Chim. Acta 1080 (2019) 146–152.
[58] Y. Cai, J.C. Niu, Y.Q. Liu, X.L. Du, Z.Y. Wu, Online sample clean-up and enrichment of proteins from salty media with dynamic double gradients on a paper fluidic channel, Anal. Chim. Acta 1100 (2020) 149–155.
[59] L. Ji, Y. Zhang, S. Yu, S. Hu, K. Wu, Morphology-tuned preparation of nanostructured resorcinol-formaldehyde carbonized polymers as highly sensitive electrochemical sensor for amaranth, J. Electroanal. Chem. 779 (2016) 169–175.
[60] N. Rasouli, N. Sohrabi, D. Ajloo, N. Rezvani, Spectroscopic, thermodynamic and molecular docking studies on interaction of toxic azo dye with bovine serum albumin, Phys. Chem. Res. 5 (2017) 541–554.